

Optical Generation and Detection of Acoustic Pulse Profiles in Gases for Novel Ultrasonic Absorption Spectroscopy

A. C. Tam and W. P. Leung^(a)

IBM Research Laboratory, San Jose, California 95193

(Received 21 May 1984)

We demonstrate a new all-optical, frequency-multiplexed, and fast technique for gas-phase ultrasonic absorption spectroscopy. A pulsed laser produces a short-duration acoustic pulse in the gas sample, and the acoustic pulse profiles at two distances are monitored by focused continuous probe beams. Fourier decompositions of these probe deflection signals provide the absorption spectrum, and examples for CO₂ and a CO₂ + H₂O mixture are given. Ultrasonic propagation speeds in the megahertz regime are also obtained for several gases.

PACS numbers: 42.60.-v, 34.50.-s, 43.85.+f

Conventional acoustic absorption spectroscopy¹⁻⁵ in gases has been performed with transducers such as quartz plates, microphones, etc. The use of transducers for gases causes several limitations. The frequency response is usually limited to ≤ 1 MHz. Also, the frequencies are scanned point by point, and the procedure is thus slow and unsuitable for transient conditions. Short-pulsed measurements are difficult because of transducer ringing. Furthermore, transducers cannot be used in hostile environments like flames. We describe here a new all-optical, pulsed, and multiplexed technique that avoids the above limitations, and is useful for acoustic absorption spectroscopy of gases. This technique relies on the use of a short-duration laser pulse to generate reliably a narrow acoustic pulse containing a broad Fourier frequency spectrum; as this pulse propagates, the various Fourier components are absorbed differently, resulting in pulse distortion that is probed by a focused cw laser beam. Fast Fourier transform of the transient probe deflection signal provides the acoustic absorption spectrum; this is much faster than the conventional pointwise frequency measurement. Our technique can be called "optoacoustic spectroscopy of the second kind" (OAS II) because it exploits optoacoustic pulse generation⁶⁻⁸ for *acoustic* spectroscopy. This should be distinguished from the well-known optoacoustic spectroscopy⁹ (understood to be the first kind), which exploits optoacoustic pulse generation for *optical* spectroscopy.

Our experimental demonstration of OAS II is shown in Fig. 1. A pulsed laser is used to generate a short-duration acoustic pulse in the gas under study. This is commonly called a pulsed optoacoustic (or photoacoustic) generation⁶ which can be achieved via many mechanisms, including simple optical absorptions and nonradiative decay,⁹ optical breakdown,¹⁰ and absorption at a solid surface with subsequent heat flow to the fluid in contact.¹¹ The experimental arrangement in Fig. 1 uses the last

mechanism, which does not require a powerful or tunable laser source, but requires an opaque target surface to be placed in contact with the gas. Here, we use a nitrogen laser beam at 337 nm with 1-mJ energy and 8-nsec duration as the pulsed excitation source. The target is a polished silicon wafer which does not absorb the gases under study, and the optically flat surface produces a plane acoustic wave front as a result of the pulsed laser heating of the Si surface. The laser spot size at the silicon surface is about 4 mm, which is much larger than the acoustic wavelengths (~ 0.3 mm at 1 MHz) in the gas presently studied, and the diffraction effect of the acoustic pulse is small. The profile and the propagation velocity of the acoustic pulse can be detected with short rise time and high spatial resolution by a tightly focused probe beam⁷ which is oriented parallel to the silicon surface (at separation x). In this way, the whole acoustic wave front arrives simultaneously at the focused probe beam,

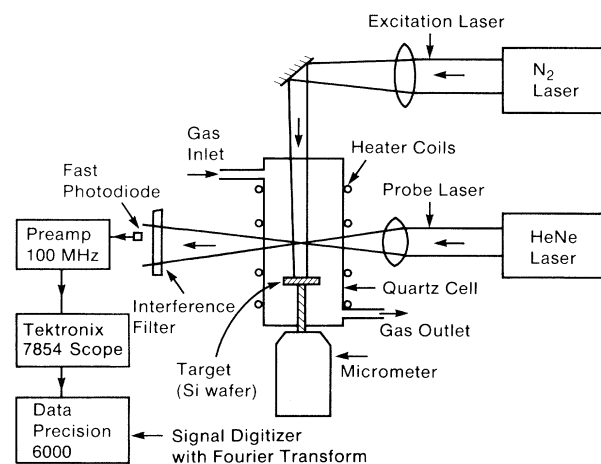


FIG. 1. Experimental arrangement for the new optoacoustic spectroscopy of the second kind. The probe-deflection signal is Fourier analyzed, and the difference between two Fourier spectra at different displacements x provides the ultrasonic absorption spectrum.

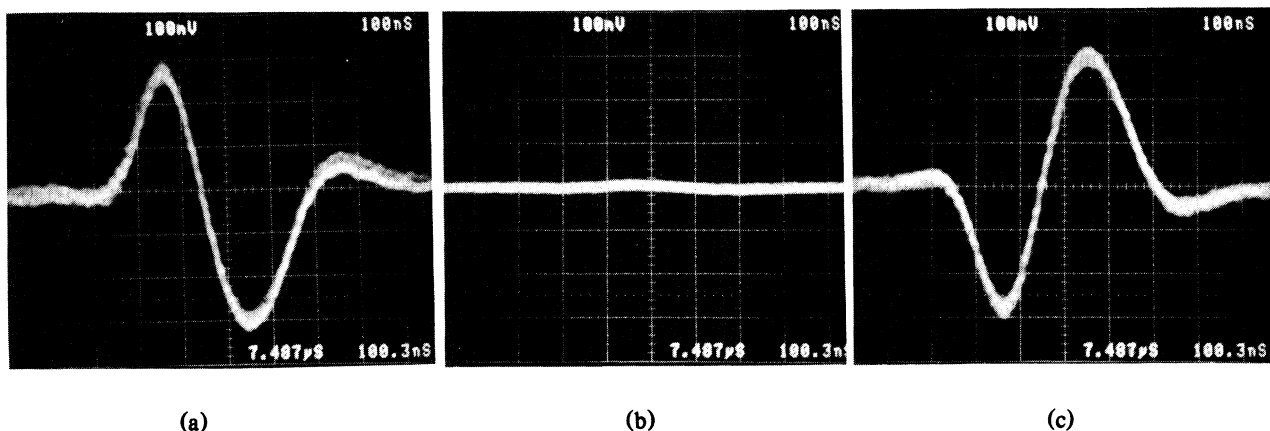


FIG. 2. Observed probe deflection signal $S(x,t)$ for dry N_2 at 22°C and $x = 2.7$ mm. The photodiode is located at one wing, at center, and at the other wing of the probe-beam cross section for (a), (b), and (c), respectively. Each scope picture is delayed by $7.487 \mu\text{s}$ from the laser pulse, and the horizontal scale is 100 ns/division .

causing a transient angular deflection $\phi(t)$ which is uniform across the probe cross section if the spatial extent of the acoustic pulse is much larger than the focused probe diameter (true for our present experiment). The probe deflection $\phi(t)$ is linearly converted into an intensity-variation signal $S(x,t)$ by a fast photodiode of small active area located where the probe beam cross-sectional area is much larger. The photodiode and preamplifier assembly we used (Analogy Modules model LNVA-O-S-100 MHz) has a bandwidth of 100 MHz . The output signal $S(x,t)$ is further amplified by a Tektronix 7854 scope with a 7A24 plugin [which also provides a single-shot display of $S(x,t)$], and then accumulat-

ed on a transient recorder (Data Precision model 6000 with model 620 plugin of bandwidth 30 MHz). Typically, $S(x,t)$ can be digitized for a single laser shot, or averaged for several laser shots for signal/noise improvement. A built-in fast Fourier transform feature in the transient recorder allows us to obtain the Fourier spectrum $\tilde{S}(x,\omega)$ of the probe beam deflection signal $S(x,t)$, where ω is an angular frequency. The above measurement is repeated with the separation between the probe beam and the silicon target changed (by a micrometer with $2\text{-}\mu\text{m}$ precision) to x' , obtaining another Fourier spectrum $\tilde{S}(x',\omega)$ corresponding to the probe-beam deflection signal $S(x',t)$. This stepwise mea-

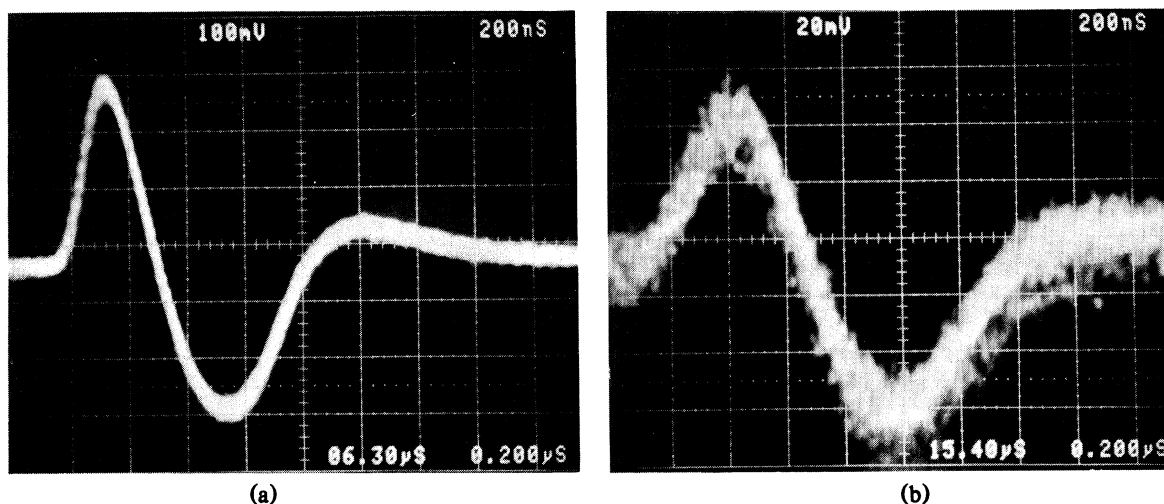


FIG. 3. Observed probe deflection signal $S(x,t)$ for $\text{CO}_2 + 20\text{-Torr H}_2\text{O}$ at 1 atm total pressure and 22°C . (a) $x = 1.816 \text{ mm}$ and scope delay time is $6.30 \mu\text{s}$; (b) $x = 4.356 \text{ mm}$ and scope delay time is $15.40 \mu\text{s}$. Horizontal scale is 200 ns/division for both.

TABLE I. Some ultrasonic velocities in gases at 1 atm and 22 °C, measured by optical acoustic pulse generation and detection.

Gas	Pure gas		Gas + 20-Torr H ₂ O	
	Mean frequency (MHz)	Acoustic velocity (10 ⁴ cm/s)	Mean frequency (MHz)	Acoustic velocity (10 ⁴ cm/s)
Ar	2.5	3.218(3)	1.5	3.240(8)
N ₂	2.5	3.512(5)	1.5	3.526(6)
O ₂	2.5	3.295(5)	1.5	3.312(5)
CF ₂ Cl ₂	0.7	1.504(10)	0.7	1.524(10)
CO ₂	2.5	2.796(3)	1.0	2.752(6)

surement at two separations is presently used to derive the ultrasonic absorption spectrum. A much faster measurement is possible by use of two probe beams¹² at separations x and x' from the target surface for single-shot detection of the deflections.

As described in a recent optoacoustic pulse-profile study in liquids,⁷ the present probe-beam deflection signal $S(x,t)$ is related to the local acoustic pressure $P(x,t)$ [with Fourier transform $\tilde{P}(x,\omega)$] by

$$S(x,t) = K \partial P(x,t) / \partial t, \quad (1)$$

where K is a constant depending on geometry, physical properties of the gas, and detection sensitivity. Fourier transform of Eq. (1) yields

$$\tilde{S}(x,\omega) = Ki\omega \tilde{P}(x,\omega), \quad (2)$$

where i is the imaginary unit. The pressure amplitude $\tilde{P}(x,\omega)$ propagates with a frequency-dependent absorption coefficient $\alpha(\omega)$ and velocity $v(\omega)$, and so we write

$$\tilde{P}(x,\omega) = \tilde{P}(0,\omega) e^{-\alpha(\omega)x + i\omega x/v(\omega)}. \quad (3)$$

Combining Eqs. (1)–(3), we have

$$\frac{\partial \ln[\text{mag}\tilde{S}(x,\omega)]}{\partial x} = -\alpha(\omega), \quad (4)$$

where $\text{mag}[\tilde{S}(x,\omega)]$ is the magnitude of the Fourier transform of $S(x,t)$.

The signal $S(x,t)$ is as given by Eq. (1) only for a sufficiently small size of the detector in the direction of beam deflection, e.g., this size should be $\leq 10\%$ of the diameter of the probe beam at the detector position. In such a case, the shape of $S(x,t)$ critically depends on the detector position, as in our case shown in Fig. 2. $S(x,t)$ is observed to change phase when detected at opposite wings of the probe beam in the far field, indicating that the probe deflection mainly occurs at the focused probe-beam region where its diameter is much smaller than the acoustic pulse width. Further data

are taken with the detector located for maximum signal amplitude.

The delay time t_d with respect to the firing of the laser indicated in Fig. 2 is measured for several path lengths x for several gases at 22 °C. We find that x changes linearly with t_d , and the gradient is the velocity v at the mean Fourier frequency f_m of the acoustic pulse. Some results are given in Table I. For the gases studied at 1 atm and 22 °C [Ar, N₂, O₂, CO₂, CF₂Cl₂ (i.e., Freon 12), and their mixtures with 20 Torr of water vapor], f_m is ~ 1 MHz, which is larger than the dispersive frequencies in the gases studied (except the mixture of CO₂ or Freon with H₂O), so that the data in Table I are the ultrasonic velocities in the “high-frequency limits.”

While the observed signals $S(x,t)$ for Ar, N₂, O₂, or their mixtures with water vapor do not change very much when x is changed by ~ 1 mm, we observe that $S(x,t)$ for the CO₂ + 20-Torr H₂O mix-

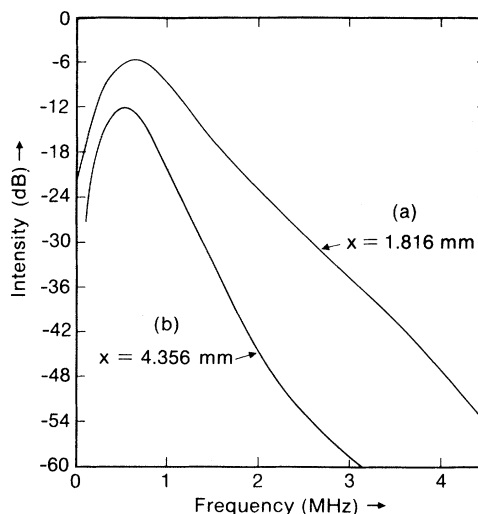


FIG. 4. Magnitude of the Fourier transform of signals in Fig. 3 as provided by the Data Precision 6000.

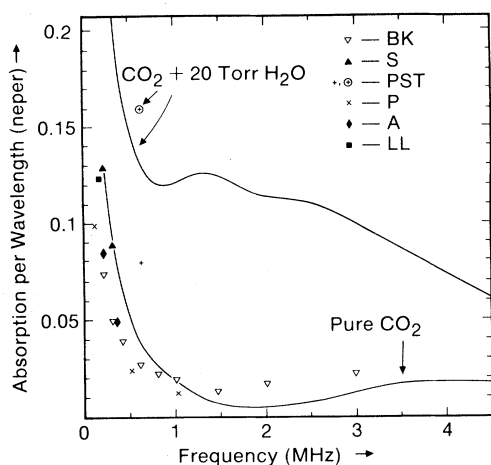


FIG. 5. Ultrasonic absorption spectra derived by the use of Eq. (4) for pure CO_2 , and for $\text{CO}_2 + 20\text{-Torr H}_2\text{O}$ at 22°C and 1 atm total pressure. Previous data for comparison are BK, Ref. 13; S, Ref. 14; PST, Ref. 15; P, Ref. 16; A, Ref. 17; LL, Ref. 18. Most of these previous data are for pure or nearly pure CO_2 , except for one indicated data point.

ture changes drastically with x , as shown in Fig. 3. As given by Eq. (4), the Fourier transforms of the signals exemplified in Fig. 4 for at least two displacements x provide the ultrasonic absorption spectrum $\alpha(\omega)$. Some results for CO_2 and $\text{CO}_2 + 20\text{-Torr H}_2\text{O}$ mixture at 22°C and 1 atm pressure are given in Fig. 5. As done traditionally, the vertical axis is absorption per wavelength, i.e., the product of $\alpha(\omega)$ and the wavelength $2\pi\nu/\omega$. Our results in Fig. 5 represent the first ultrasonic absorption spectra obtained all optically in a Fourier-multiplexed manner. Previous results were obtained by pointwise frequency measurement with the use of transducers for generation and detection; the long rise times of most transducers is a reason why high-frequency data are lacking in Fig. 5. It is already well known^{1,2} that "relaxational absorption" of sound at frequency ω occurs for an inelastic collisional rate on the order of ω ; this is probably the reason for the large absorption feature for the CO_2 and H_2O mixture in the range ~ 1 to 5 MHz. The inelastic cross section for H_2O and CO_2 collision is unusually large (close to geometrical cross section), and the inelastic collisional rate for the $\text{CO}_2/\text{H}_2\text{O}$ mixture studied is $\sim 10^7 \text{ sec}^{-1}$. Such re-

laxational ultrasonic absorption at lower H_2O concentration (corresponding to lower frequency absorption) has been observed previously.^{13,19,20}

This work is supported in part by the Office of Naval Research. We are indebted to H. Coufal for very helpful discussions.

(a)Present and permanent address: Department of Physics, Chinese University of Hong Kong, Shatin (New Territory), Hong Kong.

¹R. B. Lindsay, in *Physical Acoustics*, edited by W. P. Mason and R. N. Thurston (Academic, New York, 1982), Vol. 16, p. 1.

²K. F. Herzfeld and T. A. Litovitz, *Absorption and Dispersion of Ultrasonic Waves* (Academic, New York, 1959).

³C. R. Petts and H. K. Wickramasinghe, *Electron. Lett.* **16**, 9 (1980).

⁴A. J. Zuckerwar and R. W. Meredith, *J. Acoust. Soc. Am.* **71**, 67 (1982).

⁵H. E. Bass, F. D. Shields, and W. D. Breshears, *J. Chem. Phys.* **79**, 5733 (1983).

⁶A. C. Tam and H. Coufal, *J. Phys. (Paris), Colloq.* **44**, C6-437 (1983).

⁷B. Sullivan and A. C. Tam, *J. Acoust. Soc. Am.* **75**, 437 (1984).

⁸M. K. Sigrist and F. K. Kneubuhl, *J. Acoust. Soc. Am.* **64**, 1652 (1978).

⁹C. K. N. Patel and A. C. Tam, *Rev. Mod. Phys.* **53**, 517 (1981).

¹⁰A. C. Tam, W. Zapka, K. Chiang, and W. Imano, *Appl. Opt.* **21**, 69 (1982).

¹¹G. C. Westel, Jr., S. A. Stotts, and C. G. Clark, *J. Phys. (Paris), Colloq.* **44**, C6-67 (1983).

¹²W. Zapka, P. Pokrowsky, and A. C. Tam, *Opt. Lett.* **7**, 477 (1981).

¹³Yu. A. Bashlachev and A. Kerimov, *Sov. Phys. Acoustics* **18**, 257 (1972).

¹⁴F. D. Shields, *J. Acoust. Soc. Am.* **29**, 450 (1957).

¹⁵W. H. Pielemeier, H. L. Saxton, and D. Telfair, *J. Chem. Phys.* **8**, 106 (1940).

¹⁶W. H. Pielemeier, *J. Acoust. Soc. Am.* **15**, 22 (1943).

¹⁷F. A. Angona, *J. Acoust. Soc. Am.* **25**, 1116 (1953).

¹⁸J. W. Lewis and K. P. Lee, *J. Acoust. Soc. Am.* **38**, 813 (1965).

¹⁹F. D. Shields, *J. Acoust. Soc. Am.* **47**, 1262 (1969).

²⁰V. O. Knudson and E. J. Fricke, *J. Acoust. Soc. Am.* **12**, 255 (1940).

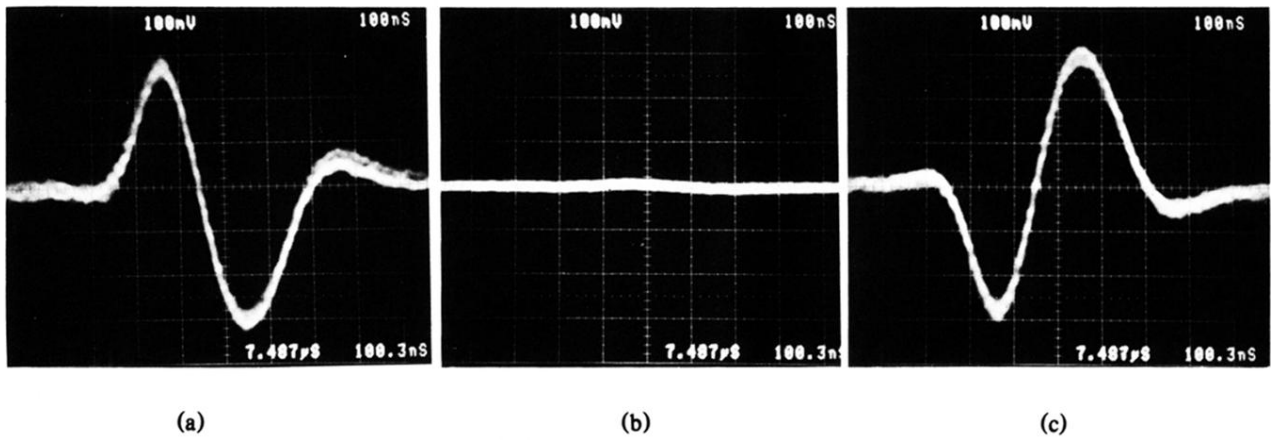


FIG. 2. Observed probe deflection signal $S(x,t)$ for dry N_2 at 22°C and $x = 2.7$ mm. The photodiode is located at one wing, at center, and at the other wing of the probe-beam cross section for (a), (b), and (c), respectively. Each scope picture is delayed by $7.487 \mu\text{s}$ from the laser pulse, and the horizontal scale is 100 ns/division .

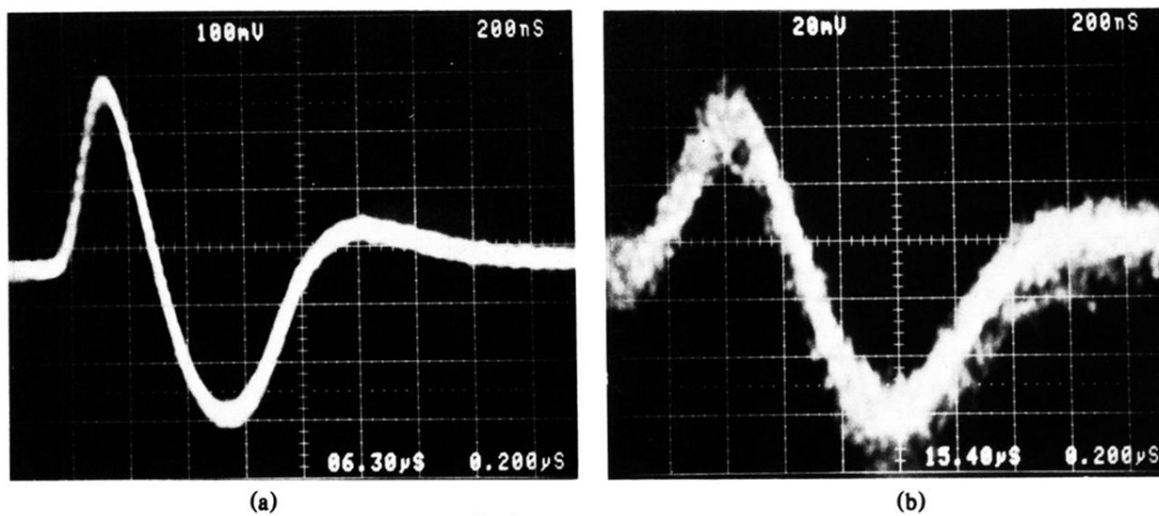


FIG. 3. Observed probe deflection signal $S(x,t)$ for $\text{CO}_2 + 20\text{-Torr H}_2\text{O}$ at 1 atm total pressure and 22°C . (a) $x = 1.816$ mm and scope delay time is $6.30 \mu\text{s}$; (b) $x = 4.356$ mm and scope delay time is $15.40 \mu\text{s}$. Horizontal scale is 200 ns/division for both.